Journal of Nuclear Medicine, published on February 16, 2017 as doi:10.2967/jnumed.113.122671

TITLE PAGE

Title

First evaluation of PET based human biodistribution and dosimetry of ^{18}F-FAZA, a tracer for imaging tumor hypoxia

Authors

Annarita Savi[1], Elena Incerti[1], Federico Fallanca[1], Valentino Bettinardi[1], Francesca Rossetti[2], Cristina Monterisi[3], Antonia Compierchio[1], Giampiero Negri[2], Piero Zannini[2], Luigi Gianolli[1], Maria Picchio[1]

1) Nuclear Medicine Department, IRCCS San Raffaele Scientific Institute, Milan, Italy
2) Thoracic Surgery Department, IRCCS San Raffaele Scientific Institute, Milan, Italy
3) University of Milano-Bicocca, Milan, Italy

Corresponding Author:
Maria Picchio, MD
Nuclear Medicine Department, IRCCS San Raffaele Scientific Institute
Via Olgettina 60, 20132
Milan, Italy
Tel. +39 02 2643 6117
Fax. +39 02 2643 2717
E-mail: picchio.maria@hsr.it

First Author:
Annarita Savi, MSc
Nuclear Medicine Department, IRCCS San Raffaele Scientific Institute
Via Olgettina 60, 20132
Milan, Italy
Tel. +39 02 2643 2715
Fax. +39 02 2643 2717
E-mail: savi.annarita@hsr.it

Short Title: FAZA human biodistribution and dosimetry
Words Count: 4502

ABSTRACT

Fluorine-18 labelled fluoroazomycinarabinoside (^{18}F-FAZA) is a positron emission tomography (PET) biomarker for non-invasive identification of regional tumor hypoxia. Aim of the present Phase I study was to firstly evaluate in non-small cell lung cancer patients the human biodistribution and dosimetry of ^{18}F-FAZA. **Methods:** Five patients awaiting surgical resection after histologically proven or radiologically suspected non-small cell lung cancer were prospectively enrolled for the study. The patients underwent a PET/computed tomography (CT) study after the injection of 371±32 MBq of ^{18}F-FAZA. The acquisition protocol consisted of a 10-minutes dynamic imaging of the heart to calculate the activity in blood, followed by four whole body PET/CT scans, from the vertex to mid-thigh, at: 10, 60, 120 and 240-minutes post-injection. Urine samples were collected after each imaging session and at 360-minutes post-injection. Volumes of interest were drawn around visually identifiable sources organs to generate time-activity-curves (TACs). Residence time were determined from TACs and effective dose (ED) to individual organs and whole body were calculated using OLINDA/EXM 1.2 for standard male and female. **Results:** Blood clearance was characterized by a rapid distribution phase, followed by a first order elimination phase. The highest uptakes were found in muscle and liver with peaks of 42.7±5.3% and 5.5±0.6% of injected activity, respectively. The total urinary excretion was 15% of the injected activity. The critical organ was urinary bladder wall with the highest radiation-absorbed doses of 0.047±0.008 mGy/MBq and 0.067±0.007 mGy/MBq calculating on 2 and 4 hours voiding intervals. The ED for standard male and female was 0.013±0.004 mSv/MBq and 0.014±0.004 mSv/MBq depending on the voiding schedule. **Conclusion:** With respect to available literature, the biodistribution of ^{18}F-FAZA appeared to be slightly different in humans than in mice, with a low clearance in humans. Therefore, estimated organ radiation doses from animal data could exhibit a moderate underestimation. Our data showed that dosimetry of ^{18}F-FAZA, for an injection of 370 MBq of tracer, is safe for its clinical use and it is almost similar to other widely used PET ligands. In particular, the ED is not appreciably different from those obtained with other hypoxia tracers, such as ^{18}F-fluoromisonidazole (^{18}F-FMISO).

Key words

Biodistribution; dosimetry; ^{18}F-FAZA PET; hypoxia; lung cancer.

INTRODUCTION

Tumor hypoxia has been identified as a major independent prognostic factor influencing tumor progression, response to therapy and overall survival in many malignancies (*1-3*). A variety of methods to measure tumor hypoxia have been proposed. However, none of the experimental in vivo methodologies (e.g. direct oxygen measurements) are currently clinically used in cancer patients, mainly because they are invasive, technically demanding and limited to accessible tumor sites (*4*,*5*).

Among the image-based modalities for hypoxia assessment, PET and ^{18}F-FMISO is one of the most extensively studied and currently used in several cancer centers worldwide (*2*,*6*,*7*). ^{18}F-FMISO is however characterized by a relatively slow clearance from blood and non-target tissues thus resulting in a low target-to-background contrast in PET images (*5*). Consequently, next generation of nitroimidazole PET tracers, such as ^{18}F-FAZA, ^{18}F-fluoroerythronitroimidazole (^{18}F-FETNIM) and ^{18}F-2-(2-nitro-1H-imidazol-1-yl)-N-(2,2,3,3,3-pentafluoropropyl)-acetamide (^{18}F-EF5) have been investigated and developed in order to achieve a faster clearance and a better tumor-background ratio (*8*). In particular, ^{18}F-FAZA has been proposed and its hypoxia-specific uptake mechanism has been demonstrated (*5*). The advantage of ^{18}F-FAZA with respect to ^{18}F-FMISO seems to be mainly related to its kinetic properties (*9*) and has been shown to be particularly promising for clinical purpose (*10-13*).

The safety and the feasibility of ^{18}F-FAZA PET imaging has been already investigated in cancer patients showing that this technique is suitable for clinical detection of hypoxia (*3*,*10*,*12*,*14*,*15*). However, although the estimation of the ED of a new agent should be mandatory to evaluate the risk-benefit ratio of medical radiation exposure, still no data are currently available on ^{18}F-FAZA biodistribution and radiation safety.

Aim of the present Phase I study was to determine the biodistribution and to calculate the radiation-absorbed doses to various organs and to the whole body for ^{18}F-FAZA in humans, by using data obtained from PET imaging of patients affected by non-small cell lung cancer.

MATERIAL AND METHODS

Subjects

Biodistribution data from five pre-surgical non-small cell lung cancer patients (2 men and 3 women; mean age: 72 years – range: 63-80 years) who underwent a whole body ^{18}F-FAZA PET/CT study at San Raffaele Scientific Institute between March 2015 to November 2015 were used for dosimetry analysis. All patients signed an informed consent prior to study participation, according to the Declaration of Helsinki and the protocol was approved by the local Ethical Committee (EudraCT number: 2011-002647-98).

Radiopharmaceutical preparation

The nucleophilic substitution reaction of no-carrier-added ^{18}F-fluoride with 1-(2,3-di-O-acetyl-5-O-tosyl-D-arabinofuranosyl)-2-nitroimidazole as precursor was performed (*16*). ^{18}F-fluoride was produced using a Cyclone 18/9 IBA cyclotron (E= 18 MeV) or a Siemens Cyclotron (11 MeV) for irradiation of ~2 mL enriched ^{18}O water (Cambridge) through the ^{18}O (p, n) ^{18}F nuclear reaction. The radiosynthesis of ^{18}F-FAZA was automatically performed with the use of a synthesis module (TRACERlab FXF-N, GE Healthcare). In the first step of the synthesis, ^{18}F-fluoride was separated from ^{18}O water using an anion exchange cartridge (preconditioned Sep-Pak Light QMA Cartridge ®, ABX). To elute the ^{18}F-fluoride

absorbed on the resin, a mixture of 0.5 mL of a solution of K_2CO_3 in water (6 mg/mL) and 1 mL of Kryptofix 222 ® (20 mg/mL) in CH_3CN was used. The solution in the reactor was then dried under vacuum at 60°C for 5 minutes and then at 120 °C for other 5 minutes. Labelling was carried out using 5 mg of the precursor dissolved in 1 mL of anhydrous DMSO under stirring at 100 °C for 5 minutes. To remove acetyl groups, basic hydrolysis was achieved with 1 mL of 0.1N NaOH at 35°C in about 2 minutes. Neutralization was performed by adding 0.5 mL of 0.5N aqueous NaH_2PO_4. The reaction mixture was mixed with a volume of 2 mL of HPLC eluent (H_2O: EtOH 98:2 (v/v)) and then passed through an Al_2O_3 cartridge (Waters) where unreacted fluorine was adsorbed. The mixture was injected onto the semipreparative HPLC column Hypersil BDS C18 (CPS Analitica) to separate the reaction product from other impurities. At a flow rate of 4 mL/minute, the product had a retention time of ~34 minutes, detected with a detector UV in series with a Geiger Muller radiodetector. The collected radiopharmaceutical was filtered using a 0.22 μm sterile filter (Minisart High Flow, Sartorius) and then diluted with NaCl 0.9% in order to have a final volume of 12 mL. The overall radiosynthesis time was about 70 minutes. Quality controls were performed to determine chemical, radiochemical and radionuclidic purities of the final product. ^{18}F-FAZA was obtained with an overall radiochemical yield of 20-25% (not decay corrected), radiochemical purity >99% and specific activity >37 GBq/μmol.

^{18}F-FAZA PET/CT image acquisition

^{18}F-FAZA was administered intravenously. The mean ± standard deviation (SD) administered activity to the five patients was 371±32 MBq (range: 277-427 MBq). The ^{18}F-FAZA PET scans were performed using a whole body PET/CT (Discovery-690 General Electric Medical System, Milwaukee, WI, USA) with a 15.3 cm axial field of view. Prior to each emission imaging session a whole body low dose CT was acquired for attenuation correction (120 kV 50 mAs). The emission study started with a 10 minutes dynamic scan over the thorax region including the heart. Four serial whole body PET scans, proceeded from the vertex to mid-thigh, were acquired at 10, 60, 120 and 240-minutes post-injection. The acquisition time was 3 minutes for bed position for each scan. The acquired data were iteratively reconstructed with attenuation, scatter, and random correction. Furthermore, time of flight information and point spread function model were also accounted in the reconstruction scheme. The specific parameters of the reconstructed protocol were: algorithm= 3D-OSEM, iterations= 3, subsets= 18, transaxial-post-filter= Gaussian with a full-width at half-maximum of 4 mm, and [1 4 1] weighted axial filter (“Standard" axial filter). Urines were collected for the following intervals: 0–60 minutes, 60–120 minutes, 120–240 minutes, and 240–300 minutes.

Activity quantification and dose calculation

To evaluate the activity concentration in the blood, the region of interest (ROI) was drawn in the left ventricle, once reoriented along the short axis of the heart where a TAC was obtained from the 10 minutes dynamic imaging and the four whole body PET/CT studies. ROIs were drawn on the fused PET/CT data for the organs that showed uptake of ^{18}F-FAZA, including brain, heart, lungs, liver, spleen, heart, muscle and intestine. All ROIs were manually drawn on the transverse slices of the first PET scan images with reference to CT scan slices. Then, the same ROIs were copied to the serially acquired images of each organ to form the TAC. The total activity in the lung was calculated excluding the tumor mass. The activity in the heart wall was obtained by subtracting the activity measured in the left ventricle cavity. To determine the uptake in the muscle a ROI was positioned in the upper leg muscle. The total activity for the muscle was obtained multiplying the cumulated

activity per milliliter with the skeletal mass (*17*). At each time point, the decayed radioactivity of each source organ was expressed as a percentage of the injected dose and plotted against time. Mono-exponential or bi-exponential functions were iteratively fitted to each source organ's decay-corrected TAC using a nonlinear least-squares regression algorithm (MATLAB Software, version 7.0, Natick, Massachusetts, USA). For each organ, the area under each TAC, from zero to infinity, was equivalent to the residence time (in hours). Due to the absence of any detectable uptake of ^{18}F-FAZA in vertebral bodies, the cumulated activity in the red marrow was calculated by an indirect assessment of the activity in the circulating blood (*18*).

Cumulative urine activity curves were generated for each patient and the accumulated radioactivity in the urine was estimated by fitting the measured data with the empiric formula $A_u\,(1\text{-}e^{-\lambda t})$ where A_u is the fraction of the injected activity excreted in the urine and λ is the clearance rate coefficient (*19*). The residence time of the urinary bladder was determined using the dynamic bladder model in OLINDA/EXM 1.2 (Organ Level Internal Dose Assessment/Exponential Modeling computer software; Vanderbilt University, 2003) (*20*). Voiding intervals of 2 and 4 hours were used to calculate different residence times to determine their effect on dose estimates to the urinary bladder wall.

Cumulated activity in the remainder of the body was calculated as follows:

$$A_{RB} = A_0 \int_0^T e^{-ln2/T_{1/2}\,t}\,dt + A_T \int_T^\infty e^{-ln2/T_{1/2}\,t}\,dt - \sum_i A_i$$

where A_{RB} is the cumulated activity in the remainder of the body, A_0 is the injected dose, A_T is the injected dose minus the excreted activity, $T_{1/2}$ is the effective half-life and A_i is the cumulated activity in the measured source organ.

The area under each TAC for each organ from zero to infinity was equivalent to the residence time (in hours). The internal radiation dosimetry for each

was evaluated using the Medical Internal Radiation Dose (MIRD) schema (*21*) with the OLINDA/EXM 1.2 software for standard male and standard female phantom. The ED and effective dose equivalent (EDE) were calculated and averaged for all the five patients.

RESULTS

Patient characteristics are documented in Table 1. After injection of ^{18}F-FAZA no adverse events were observed. In Figure 1 a representative case of a whole body ^{18}F-FAZA biodistribution at various intervals is shown. At 10 minutes (start time of the first whole-body acquisition) the main regions showing ^{18}F-FAZA uptake are: heart, blood, liver, spleen, urinary bladder, renal cortex, and muscle. In this early image the uptake of the tumor mass in the right lung, is clearly visible. Due to the rapid clearance from the blood in the delayed images the activity in the blood and spleen is not visible, while liver, muscle and renal cortex are clearly visualized and contain more radioactivity than the rest of the body.

Figure 2 illustrated the relative excreted ^{18}F-FAZA activity in the urine. The graph shows that up to 15% of injected activity is extracted via the urinary pathway, and this clearance is relatively rapid with 10% of the tracer excreted 90 minutes after the injection.

Figures 3 and 4 shows the mean time TACs for blood, brain, lung, liver, kidneys, spleen, intestine and muscle derived from PET imaging of the five patients. Radioactivity was excreted by kidney, with a fast clearance and hepatic metabolism. The highest uptakes were found in muscle and liver with peaks of 42.7±5.3% and 5.5±0.6% of injected activity in the whole organ, respectively. In particular, the liver to muscle ratio at 10 minutes is approximately 2.06, while at 60, 120 and 240 minutes it is 1.47, 1.65 and 1.47, respectively.

The residence times of ^{18}F-FAZA for the considered organs are shown in Table 2. To explain the great difference between liver and muscle residence time the different masses of the organ has to be take in account. For a reference human phantom of 70 Kg, the liver has a weight of 1.9 Kg while for the muscle the weight is 21 and 33 kg for female and male, respectively (*17*). The radiation dose estimates is shown in Table 3 expressed as mean ± SD. The highest radiation-absorbed dose were found for the urinary bladder wall, with 0.05 mGy/MBq or 0.07 mGy/MBq corresponding to 2 or 4 hours voiding intervals. The different voiding schedule, resulted in similar absorbed doses for other organs. The ED was 0.013 mSv/MBq and 0.014 mSv/MBq resulting in a radiation dose of 4.8 or 5.2 mSv for 370 MBq injection of ^{18}F-FAZA depending on the voiding schedule. In our series of patients, ^{18}F-FAZA tracer injection was well tolerated, and no pharmacological side effects were observed.

DISCUSSION

In the current study biodistribution and dosimetry of ^{18}F-FAZA was determined for the first time in humans. Previously, Piert et al. (*5*) and Reischl et al. (*22*) have reported biodistribution data in animal models. They reported the highest ^{18}F-FAZA uptake in the liver and muscle kidneys while relatively low uptakes were observed in lung, heart, muscle and brain (*5*). These previous findings are in accordance with the results reported in the present study. However, in humans, a slower clearance in liver and kidney with respect to those obtained in animals ($T_{1/2}$ = 32 minutes vs 3 minutes for liver and $T_{1/2}$= 30 minutes vs 5 minutes for kidney) was shown while the clearance in the muscle tissue was comparable. The half-time in animals were derived from biodistribution data at 10, 60 and 180 minutes after administration in nude mice (*5*). These findings are probably due to the faster physiology of rodents in kidneys and liver. Therefore, using data derived from preclinical studies to estimate the human ED might lead to an underestimation of this parameter.

^{18}F-FMISO was one of the first PET tracers used for imaging tumor oxygenation (*19*). Nevertheless, ^{18}F-FMISO shows several disadvantages. Limitations of this radiotracer include slow tracer accumulation, slow plasma clearance and low tumor-to-background contrast requiring delayed scans to allow background activity to decrease (*23*): ^{18}F-FMISO imaging usually requires an interval longer than 2 hours (ideally 4 hours) after administration.

To overcome these limitations other nitroimidazole PET tracers with high avidity for hypoxic tissue have been investigated and developed, including ^{18}F-FETNIM (*24*), which is more hydrophilic than ^{18}F-FMISO and can be washed out more rapidly from normal oxygenated tissues, theoretically allowing a higher tumor-to-background ratio (*8*). In addition, another hypoxia tracer, with a more stable but also more complex labeling chemistry, is represented by ^{18}F-EF5 (*8*,*25*,*26*). This tracer is slightly more lipophilic than the formerly described compounds and have been investigated in animal models and in clinical studies in different tumors (*26*). For these tracers the optimal tumor-to-muscle cut-off value is low (1.5) and the potential advantage over ^{18}F-FMISO is still negligible (*8*). Comparing the different nitroimidazole tracers, ^{18}F-FAZA, ^{18}F-EF5 and ^{18}F-FETNIM are characterized by a more hydrophilic than ^{18}F-FMISO, thus providing a faster diffusion into cells, making it more readily available for specific reductive retention in hypoxic cells *(9,27)*.

Postema et al. (*15*) provided estimation on the EDE in man and female and uptake values in different organs at 2 hours after ^{18}F-FAZA administration (*5*). However, biodistribution data and doses to target organs were not reported.

To our knowledge this is the first paper presenting a comprehensive ^{18}F-FAZA dosimetry in humans. Comparing our data with the available literature on ^{18}F-FMISO, ^{18}F-FETNIM and ^{18}F-EF5 (Table 3), we found that the EDE of ^{18}F-FAZA

(0.015 mSv/MBq) is slightly higher than ^{18}F-FMISO (0.013 mSv/MBq) (*19*). The greater differences in radiation-absorbed doses were seen in urinary bladder (0.047, 0.021, 0.062 and 0.017 mGy/MBq for ^{18}F-FAZA, ^{18}F-FMISO, ^{18}F-FETNIM and ^{18}F-EF5, respectively). This is related the urinary excretion rate much faster for ^{18}F-FETNIM with the 60% of injected activity cleared trough the urinary pathway, while only 3%, 15% and 16% of injected activity was excreted with ^{18}F-FMISO, ^{18}F-FAZA, and ^{18}F-EF5, respectively. We found that the EDE of ^{18}F-FAZA (0.015mSv/MBq) is between the values obtained with ^{18}F-FETNIM (0.017 mSv/MBq) and ^{18}F-FMISO (0.013 mSv/MBq), while ^{18}F-EF5 show EDE of 0.029 mSv/MBq. The higher doses of ^{18}F-EF5, both for urinary bladder and EDE is probably due to the Authors assumption in the evaluation of doses, that no activity was excreted (*26*).

^{18}F-FAZA PET/CT is a valuable tool in oncological patients as prognostic biomarker (*28*) and as guide to tailored treatments, such as hypoxia-directed intensity modulated radiotherapy approaches (*14*,*29*). The results of our analysis show a favorable radiation risk profile associated to a whole body PET with ^{18}F-FAZA, thus being ^{18}F-FAZA PET/CT feasible for clinical hypoxia evaluation and also allowing patients to safely receive consecutive PET/CT studies, if clinically required.

CONCLUSION

The first biodistribution and internal dosimetry profiles in human following administration of ^{18}F-FAZA have been presented. The favorable radiation risk profile associated to whole-body ^{18}F-FAZA PET is definitely feasible for clinical hypoxia evaluation, also allowing patients to safely undergo more PET/CT studies.

CONFLICT OF INTEREST

Authors declare that they have no conflict of interest.

ACKNOWLEDGMENTS

This work was supported by the Italian Ministry of Health, Ricerca Finalizzata GR-2009-1575612.

REFERENCES

1. Cherk MH, Foo SS, Poon AM, et al. Lack of correlation of hypoxic cell fraction and angiogenesis with glucose metabolic rate in non-small cell lung cancer assessed by 18F-Fluoromisonidazole and 18F-FDG PET. *J Nucl Med.* 2006;47:1921-1926.

2. Lewis JS, Welch MJ. PET imaging of hypoxia. *Q J Nucl Med.* 2001;45:183-188.

3. Souvatzoglou M, Grosu AL, Roper B, et al. Tumour hypoxia imaging with [18F]FAZA PET in head and neck cancer patients: a pilot study. *Eur J Nucl Med Mol Imaging.* 2007;34:1566-1575.

4. Bollineni VR, Kerner GS, Pruim J, et al. PET imaging of tumor hypoxia using 18F-fluoroazomycin arabinoside in stage III-IV non-small cell lung cancer patients. *J Nucl Med.* 2013;54:1175-1180.

5. Piert M, Machulla HJ, Picchio M, et al. Hypoxia-specific tumor imaging with 18F-fluoroazomycin arabinoside. *J Nucl Med.* 2005;46:106-113.

6. Eschmann SM, Paulsen F, Bedeshem C, et al. Hypoxia-imaging with (18)F-Misonidazole and PET: changes of kinetics during radiotherapy of head-and-neck cancer. *Radiother Oncol.* 2007;83:406-410.

7. Laforest R, Dehdashti F, Lewis JS, Schwarz SW. Dosimetry of 60/61/62/64Cu-ATSM: a hypoxia imaging agent for PET. *Eur J Nucl Med Mol Imaging.* 2005;32:764-770.

8. Lopci E, Grassi I, Chiti A, et al. PET radiopharmaceuticals for imaging of tumor hypoxia: a review of the evidence. *Am J Nucl Med Mol Imaging.* 2014;4:365-384.

9. Sorger D, Patt M, Kumar P, et al. [18F]Fluoroazomycinarabinofuranoside (18FAZA) and [18F]Fluoromisonidazole (18FMISO): a comparative study of their selective uptake in hypoxic cells and PET imaging in experimental rat tumors. *Nucl Med Biol.* 2003;30:317-326.

10. Halmos GB, Bruine de Bruin L, Langendijk JA, van der Laan BF, Pruim J, Steenbakkers RJ. Head and neck tumor hypoxia imaging by 18F-fluoroazomycin-arabinoside (18F-FAZA)-PET: a review. *Clin Nucl Med.* 2014;39:44-48.

11. Bollineni VR, Koole MJ, Pruim J, et al. Dynamics of tumor hypoxia assessed by 18F-FAZA PET/CT in head and neck and lung cancer patients during chemoradiation: possible implications for radiotherapy treatment planning strategies. *Radiother Oncol.* 2014;113:198-203.

12. Trinkaus ME, Blum R, Rischin D, et al. Imaging of hypoxia with 18F-FAZA PET in patients with locally advanced non-small cell lung cancer treated with definitive chemoradiotherapy. *J Med Imaging Radiat Oncol.* 2013;57:475-481.

13. Havelund BM, Holdgaard PC, Rafaelsen SR, et al. Tumour hypoxia imaging with 18F-fluoroazomycinarabinofuranoside PET/CT in patients with locally advanced rectal cancer. *Nucl Med Commun.* 2013;34:155-161.

14. Grosu AL, Souvatzoglou M, Roper B, et al. Hypoxia imaging with FAZA-PET and theoretical considerations with regard to dose painting for individualization of radiotherapy in patients with head and neck cancer. *Int J Radiat Oncol Biol Phys.* 2007;69:541-551.

15. Postema EJ, McEwan AJ, Riauka TA, et al. Initial results of hypoxia imaging using 1-alpha-D: -(5-deoxy-5-[18F]-fluoroarabinofuranosyl)-2-nitroimidazole (18F-FAZA). *European journal of nuclear medicine and molecular imaging.* 2009;36:1565-1573.

16. Reischl G, Ehrlichmann W, Bieg C, et al. Preparation of the hypoxia imaging PET tracer [18F]FAZA: reaction parameters and automation. *Appl Radiat Isot.* 2005;62:897-901.

17. Janssen I, Heymsfield SB, Wang ZM, Ross R. Skeletal muscle mass and distribution in 468 men and women aged 18-88 yr. *J Appl Physiol (1985).* 2000;89:81-88.

18. Sgouros G. Bone marrow dosimetry for radioimmunotherapy: theoretical considerations. *J Nucl Med.* 1993;34:689-694.

19. Graham MM, Peterson LM, Link JM, et al. Fluorine-18-fluoromisonidazole radiation dosimetry in imaging studies. *J Nucl Med.* 1997;38:1631-1636.

20. Stabin MG, Sparks RB, Crowe E. OLINDA/EXM: the second-generation personal computer software for internal dose assessment in nuclear medicine. *J Nucl Med.* 2005;46:1023-1027.

21. Stabin MG. MIRDOSE: personal computer software for internal dose assessment in nuclear medicine. *J Nucl Med.* 1996;37:538-546.

22. Reischl G, Ehrlichmann W, Bieg C, et al. Preparation of the hypoxia imaging PET tracer [18F]FAZA: reaction parameters and automation. *Appl Radiat Isot.* 2005;62:897-901.

23. Yip C, Blower PJ, Goh V, Landau DB, Cook GJ. Molecular imaging of hypoxia in non-small-cell lung cancer. *Eur J Nucl Med Mol Imaging.* 2015;42:956-976.

24. Tolvanen T, Lehtio K, Kulmala J, et al. F-18-fluoroerythronitroimidazole radiation dosimetry in cancer studies. *J Nucl Med.* 2002;43:1674-1680.

25. Lin LL, Silvoniemi A, Stubbs JB, et al. Radiation Dosimetry and Biodistribution of the Hypoxia Tracer F-18-EF5 in Oncologic Patients. *Cancer Biother Radio.* 2012;27:412-419.

26. Koch CJ, Scheuermann JS, Divgi C, et al. Biodistribution and dosimetry of F-18-EF5 in cancer patients with preliminary comparison of F-18-EF5 uptake versus EF5 binding in human glioblastoma. *Eur J Nucl Med Mol Imaging*. 2010;37:2048-2059.

27. Kurihara H, Honda N, Kono Y, Arai Y. Radiolabelled Agents for PET Imaging of Tumor Hypoxia. *Curr Med Chem.* 2012;19:3282-3289.

28. Mortensen LS, Johansen J, Kallehauge J, et al. FAZA PET/CT hypoxia imaging in patients with squamous cell carcinoma of the head and neck treated with radiotherapy: results from the DAHANCA 24 trial. *Radiother Oncol.* 2012;105:14-20.

29. Ling CC, Humm J, Larson S, et al. Towards multidimensional radiotherapy (MD-CRT): biological imaging and biological conformality. *Int J Radiat Oncol Biol Phys.* 2000;47:551-560.

FIGURES LEGENDS

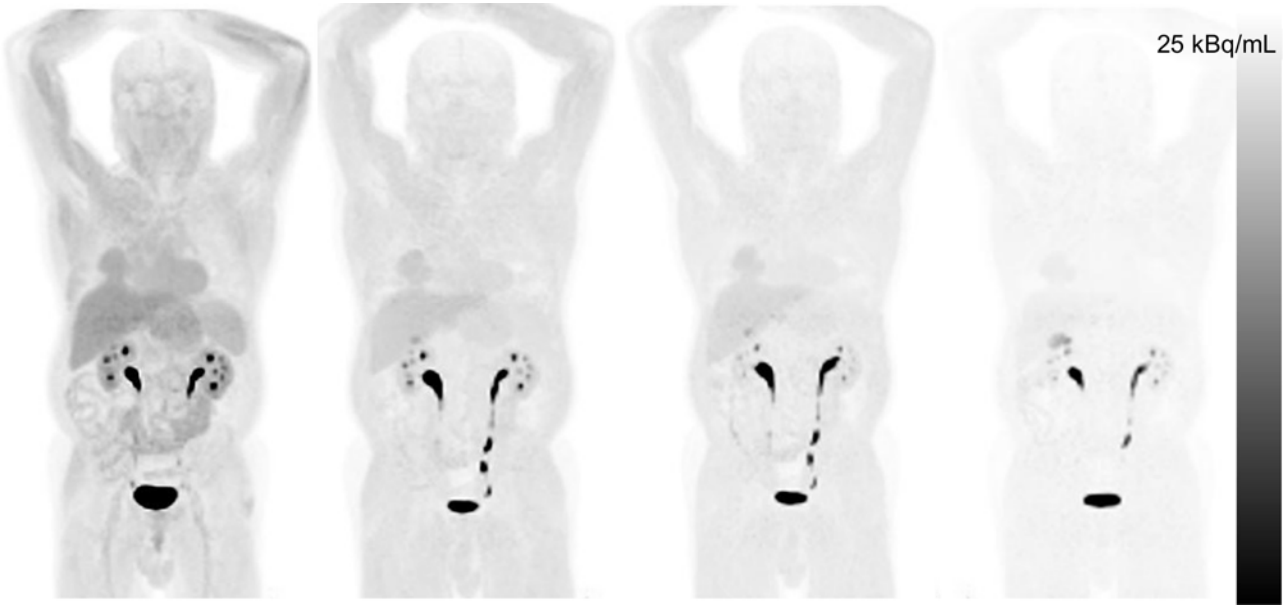

Figure 1

Collapsed coronal images of a representative patient following administration of ^{18}F-FAZA acquired at (left to right) 10, 60, 120, 240 minutes post injection.

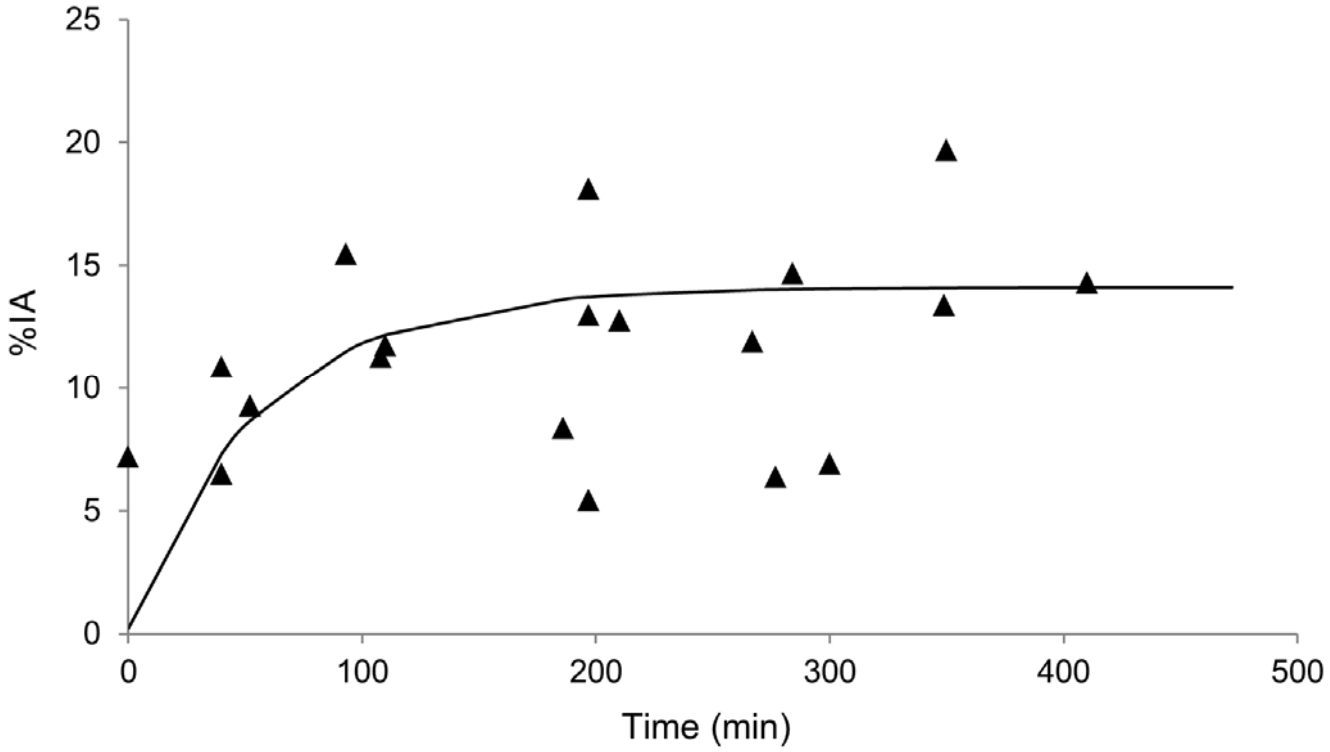

Figure 2
^{18}F-FAZA urine activity expressed as % of injected activity (IA). The solid line represent the best fit of 19 sample from 5 patients.

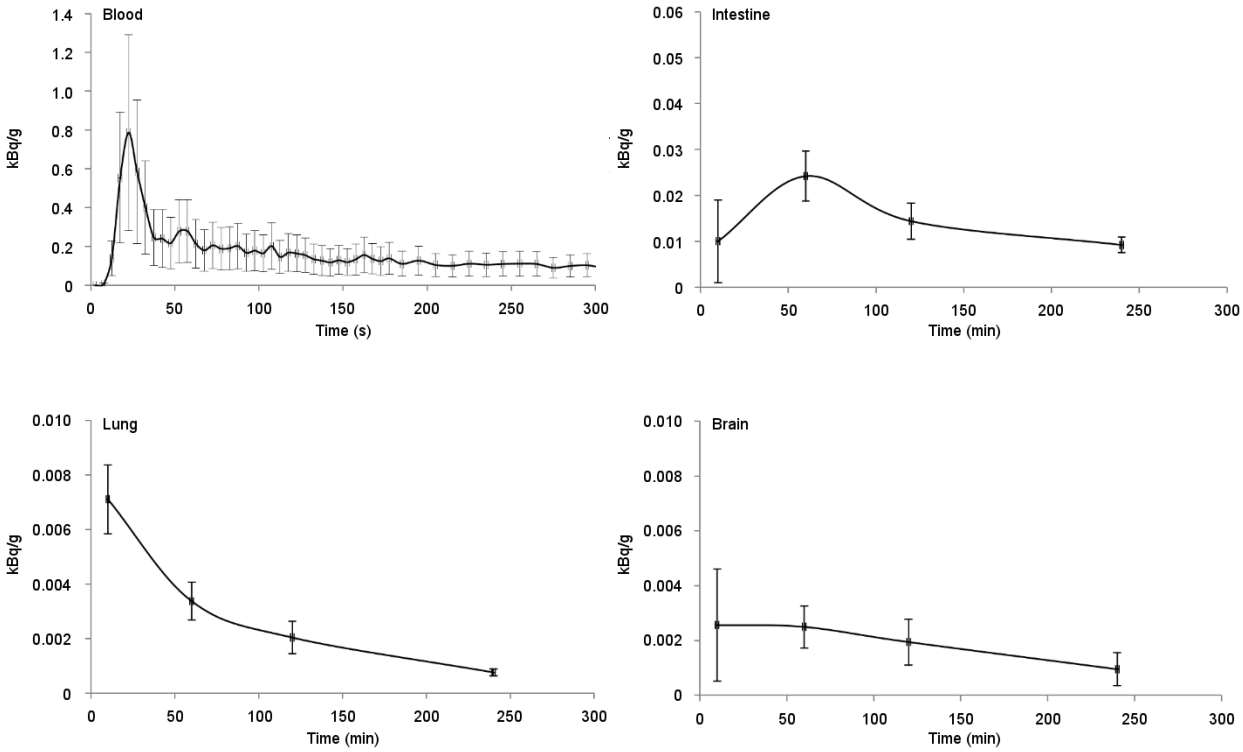

Figure 3

Time activity curves in blood (heart chamber), intestine, lung, and brain. Activity has been normalized to 1 MBq injected activity and standard male and female. Data represent mean ± SD of results from five patients.

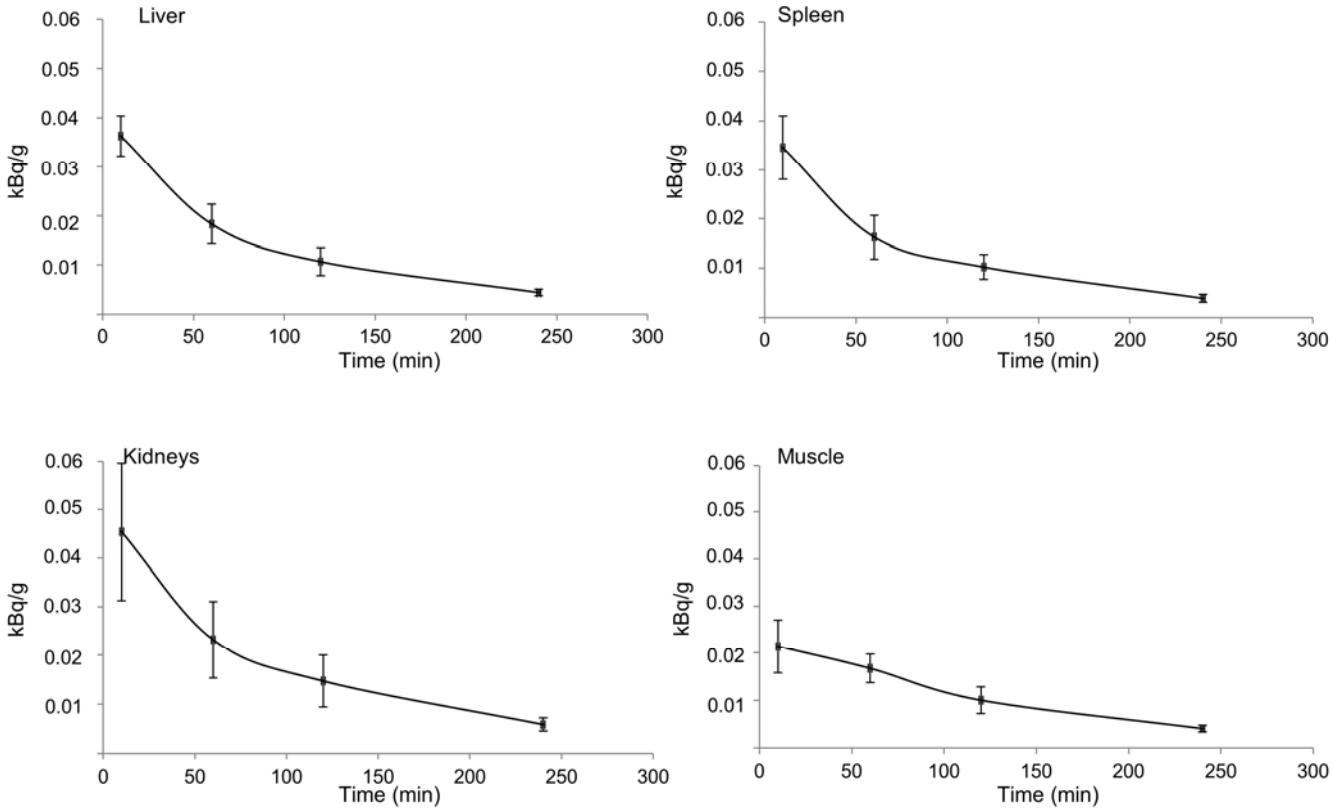

Figure 4

Time activity curves in liver, spleen, kidneys and muscle. Activity has been normalized to 1 MBq injected activity. Data represent mean ± SD of results from five patients.

TABLES

Table 1. Patient Characteristics

Gender	Male/Female	**2/3**
Age	Mean (years; range)	**72 (63-80)**
Body Weight	Mean (kg; range)	**60 (49-74)**
Injected dose	Mean ± SD* (MBq; range)	**371±32 (277-427)**
Histology	Adenocarcinoma	**5**
Stage	I A-B	**4**
	III A	**1**
Local Extension	pT1-T2	**4**
	pT3	**1**
	pN0	**4**
	pN1	**1**
	Mx	**5**
Grade	G2	**3**
	G3	**2**

*SD: Standard Deviation

Table 2. Residence Times (Mean ± SD, n= 5 patients) of ^{18}F-FAZA for Measured Source Organs

Source Organ	Time (hour)
Brain	0.014 ± 0.002
Gall-bladder content	0.019 ± 0.001
Intestine	0.013 ± 0.005
Heart content	0.018 ± 0.002
Kidneys	0.025 ± 0.003
Liver	0.110 ± 0.019
Lungs	0.036 ± 0.011
Muscle	1.090 ± 0.180
Red Marrow	0.034 ± 0.005
Spleen	0.011 ± 0.003
Urinary Bladder content 2h	0.055 ± 0.009
Urinary Bladder content 4h	0.081 ± 0.008
Remainder 2h	1.130 ± 0.320
Remainder 4h	1.100 ± 0.310

Table 3. Absorbed Doses (Mean ± SD, n= 5 patients) of ^{18}F-FAZA to Target Organs

Tracers	Voiding interval				
	^{18}F-FAZA		**^{18}F-FMISO (*19*)**	**^{18}F-FETNIM (*24*)**	**^{18}F-EF5 (*26*)**
Target Organ	2h (mGy/MBq)	4h (mGy/MBq)	2h (mGy/MBq)	2h (mGy/MBq)	2.5h (mGy/MBq)
	Mean ± SD*	Mean ± SD*	Mean	Mean	Mean
Adrenals	0.012 ± 0.001	0.012 ± 0.001	0.017	0.012	0.014
Brain	0.004 ± 0.001	0.004 ± 0.001	0.009	0.006	0.012
Breasts	0.009 ± 0.001	0.009 ± 0.001	0.012	0.007	0.009
Gall-bladder Wall	0.013 ± 0.004	0.013 ± 0.004	0.015	0.014	0.055
Lower Large Intestine Wall	0.013 ± 0.006	0.013 ± 0.006	0.014	0.012	0.017
Small Intestine	0.012 ± 0.005	0.012 ± 0.005	0.013	0.012	0.015
Stomach Wall	0.012 ± 0.001	0.012 ± 0.001	0.013	0.012	0.013
Upper Large Intestine Wall	0.013 ± 0.002	0.013 ± 0.002	0.014	0.014	0.015
Heart Wall	0.018 ± 0.001	0.018 ± 0.001	0.019	0.011	0.022
Kidneys	0.017 ± 0.002	0.017 ± 0.002	0.016	0.027	0.025
Liver	0.016 ± 0.003	0.016 ± 0.003	0.018	0.024	0.023
Lungs	0.011 ± 0.008	0.011 ± 0.008	0.010	0.008	0.017
Muscle	0.011 ± 0.009	0.011 ± 0.009	0.014	0.012	0.012
Ovaries	0.014 ± 0.001	0.014 ± 0.001	0.018	0.013	0.017
Pancreas	0.013 ± 0.002	0.013 ± 0.002	0.018	0.019	0.014
Red Marrow	0.011 ± 0.001	0.011 ± 0.001	0.011	0.012	0.022
Bone Surface	0.011 ± 0.002	0.011 ± 0.002	0.008	0.011	0.021
Skin	0.008 ± 0.001	0.008 ± 0.001	0.005	0.007	0.008
Spleen	0.017 ± 0.008	0.017 ± 0.009	0.016	0.020	0.012
Thymus	0.011 ± 0.003	0.011 ± 0.001	0.016	0.009	0.011
Thyroid	0.010 ± 0.001	0.010 ± 0.001	0.015	0.009	0.011
Urinary Bladder Wall	0.047 ± 0.008	0.067 ± 0.007	0.021	0.062	0.017
Uterus	0.020 ± 0.001	0.021 ± 0.001	0.018	0.015	0.023
Testes	0.004 ± 0.001	0.005 ± 0.001	0.015	0.010	0.013
Total Body	0.012 ± 0.002	0.012 ± 0.002	0.013	0.011	0.014
Effective Dose Equivalent (mSv)	0.015 ± 0.004	0.017 ± 0.004	0.013	0.017	0.029
Effective Dose (mSv)	0.013 ± 0.004	0.014 ± 0.004	-	0.015	0.023

*SD: standard deviation